



Electron beam lithography on cylindrical roller

Shih Chun Tseng^{a,*}, Wen Yang Peng^b, Yi Fan Hsieh^c, Ping Jen Lee^a, Wen Lang Lai^b

^aNano Technology Research Center, Industrial Technology Research Institute, Hsinchu 300, Taiwan, ROC

^bMechanical and Systems Research Laboratories, Industrial Technology Research Institute, 300, Taiwan, ROC

^cDepartment of Materials Science and Engineering, National Chiao Tung University, 300, Taiwan, ROC

ARTICLE INFO

Article history:

Received 9 September 2009

Received in revised form 27 November 2009

Accepted 27 November 2009

Available online 3 December 2009

Keywords:

Electron beam lithography
Ni electroforming template
Cylindrical roller

ABSTRACT

We developed a nano-structure fabrication technology over a cylindrical roller using electron beam lithography (EBL) and a specimen rotation apparatus. The high-resolution patterning is done on a cylindrical roller specimen and it is achieved by controlling the thickness of photo-resistance (PR) and dosage of the electron beam (EB). We successfully obtained homogeneous arrays of one-third circle grating with a nano-scale width 100 nm and a large area of 6×3.5 mm square. Couples of the “ITRI” character marks were also fabricated. The stitching control was accurately derived using the in-house made two-axis rotation system, which provides the smallest stitching of about $1.6 \mu\text{m}$. The minimum feature size of 100 nm over the cylindrical roller is demonstrated. Moreover, the Nicole template with “ITRI” character pattern on the cylindrical roller was also successfully made, of which thickness is about 80 nm.

© 2009 Elsevier B.V. All rights reserved.

1. Introduction

Nano-scale materials have been attractive recently due to its high potential applications such as photonic crystal [1,2], solar system [3,4], display [5,6], and photo detector devices [7,8]. Electron beam lithography (EBL) is one of the most promising nano-scale technologies which have been introduced in recently years. The high-resolution capability and the direct-writing adaptability have added up to the EBL to play an important role in research and development of all kinds of nano-science. In addition, it has versatile functions for fabricating arbitrary-element shapes and array configurations. Although, the application targets always focus on wafers and masks that are very flat and large but not a 3D specimen. Recently, various traditional three dimensional (3D) nano-structure skills have been reported in the micro-electro-mechanical systems (MEMS) field, such as the optical or X-ray lithography [9], which is difficult to apply because the resolutions of all these approaches range from sub-micron to a few microns [10–13]. On the other hand, EBL has great advantages to develop 3D nano-structure fabrication. Few groups [14,15] have focused on the 3D specimen to create 3D nano-patterns. They have devised 3D nano-patterns over polymethylmethacrylate (PMMA) spheres by using EBL. The EBL would have widened applications in various fields of nano-world by creating 3D structures with small feature size, such as nano-imprinting [16,17]. In this study, we have developed a rotation axis (*R*-axis) driver, polisher system and photo-resist coating facility to overcome one important issue about how to

create a 3D nano-structure by EBL. The manufacturing process of the one-third circle grating structure over a roller specimen is made by an in-house-made *R*-axis drive apparatus and an electron beam lithography. The *R*-axis allows the roller specimen to be exposed by E-beam, and thus enables the creation of nano-structures. In addition, a photo-resist coating system was developed as an aid to coat uniform thickness over a cylindrical roller. The effects of the motion of the cylindrical roller on the stitching error were also investigated. In addition, couples of patterns of ITRI character marks were also fabricated, which adopted the electroforming process to shape the roller template.

2. Experimental set-up

In this study, arrays of nano-scale grating over a cylindrical roller were fabricated through a combination of the in-house-made rotation axis (*R*-axis) drive apparatus, home made roller polisher facility, in-house-made photo-resist coating system, and electron beam lithography (EBL). The *R*-axis can rotate through an angle of 360° and the *x* and *y*-axis were controlled by the system of EBL. The *R*-axis drive system is built on a pallet and equipped with its own electrical system that could be loaded into the stage of EBL. The system includes its controller, retarding motor, roller base, and data panel. The in-house made rotation axis drive apparatus has very high angular resolution. The motor and its driver satisfies the micro-scale positioning function. The data panel shows the rotation speed, tilt angle, and working time, etc. Before the polishing process, the roller was coated with an Ni layer ($150 \mu\text{m}$) by electroless plating. As to the in-house-made photo-resist coating system, there are two processes involved to prove the photo-resist

* Corresponding author.

E-mail address: sctsen@itri.org.tw (S.C. Tseng).

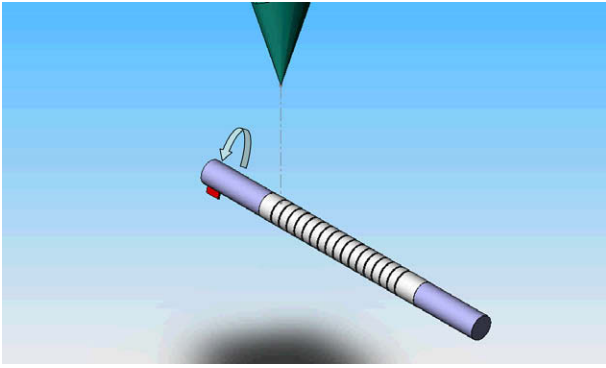


Fig. 1. Schematic of the process for fabricating nano-structure on cylindrical roller by EBL.

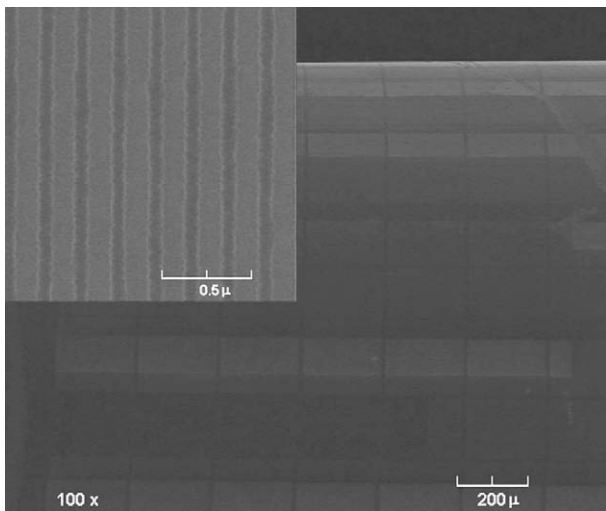


Fig. 2(a). SEM micrograph of the arrays one-third circle grating over the roller. The exposed area is 6×3.5 mm square.

coating quality. First, the non-contact floating type polishing system achieves very nice roller surface. As rotating, the polishing process was done as Al_2O_3 powder interacted with the roller. Second, in order to spread the photo-resist on the roller uniformly by

centrifugal force, a coating apparatus with ultra-high rotation speed is developed with regard to the meso-scale roller. The roller was jointed with a high speed axial rotation center (of the speed range from 15,000 r.p.m. to 25,000 r.p.m.), and followed by dropping down the photo-resist from the top of roller. The process began with coating the positive photo-resist of ZEP520, which was followed by electron beam (E-beam) exposing, and development process. To investigate the effects of the R -axis rotating on stitching error, several rotating speeds were used. E-beam exposure was used to define the location and size. The exposure of e-beam current is about 100 pA and an acceleration voltage of 30 kV. The type of EBL was CABL-2000 made by CRESTEC. The measurements of the surface structure were measured by an atomic force microscopy (AFM) and a scanning electron microscopy (SEM).

The results herein demonstrate that various dosage of EBL could fabricate different width of circle grating.

3. Results and discussions

Fig. 1 shows schematically the process flow of how the cylindrical roller specimen be exposed by EBL. In order to achieve uniformity thickness of photo-resist, two factors need to consider, one is the polishing process, and the other one is controlling stability of high speed axle center system. The microscopic images of the arrays one-third circle grating over the roller, which exposed area is 6×3.5 mm square, as shown in **Fig. 2(a)**. A couple of factors will affect the resolution of patterns such as curvature of roller, dosage of EBL, and electron scattering, during E-beam exposing. As presented in the inset of **Fig. 2(a)**, the width of arrays grating patterns is 100 nm, and the pitch is 200 nm with exposure dosage of 0.5 ms. It is also found that the grating structure has high uniformity. **Fig. 2(b)** demonstrated the thickness of photo-resist is about 305 nm by AFM. It proved the relation between dosage of EBL and resolution is positively related. Furthermore, else two influence factors are the electron forward scattering and the back scattering. The electron forward and back scattering trajectory will be changed as adjusting curvature of roller. These influence factors has cross-relationship with each other. It then adds up the difficulty to control the resolution and position of grating. The stitching error of arrays grating patterns had been measurement by AFM and the smallest value was found to be $1.6 \mu\text{m}$ by line to line, as shown in **Fig. 3**. The stitching errors were decreased from $30 \mu\text{m}$ to $1.6 \mu\text{m}$ as decreasing the height of R -axis drive stage from 4.5 mm to 0.5 mm, respectively. It means the stitching comes from the height relative to the surface of R -axis drive stage and the focus

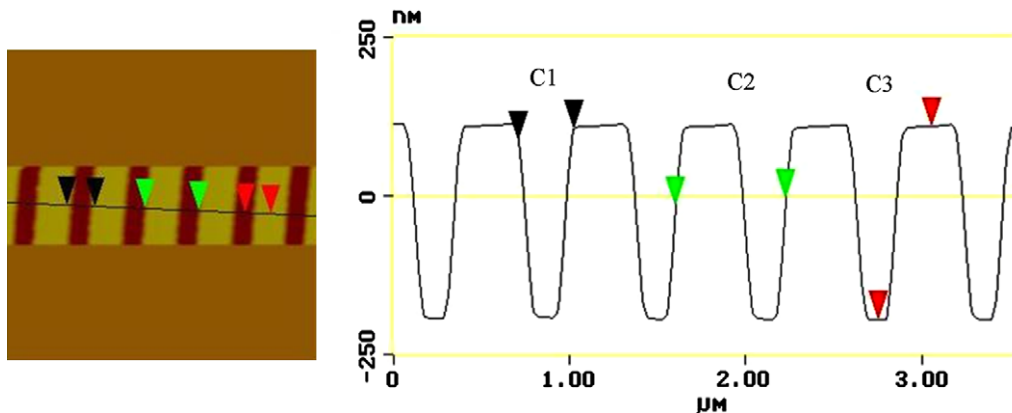


Fig. 2(b). AFM micrograph of nano-grating with the thickness of photo-resist. C1 is grating distance (309 nm), C2 is the pitch of grating (618 nm), C3 is depth of photo-resist (305 nm).

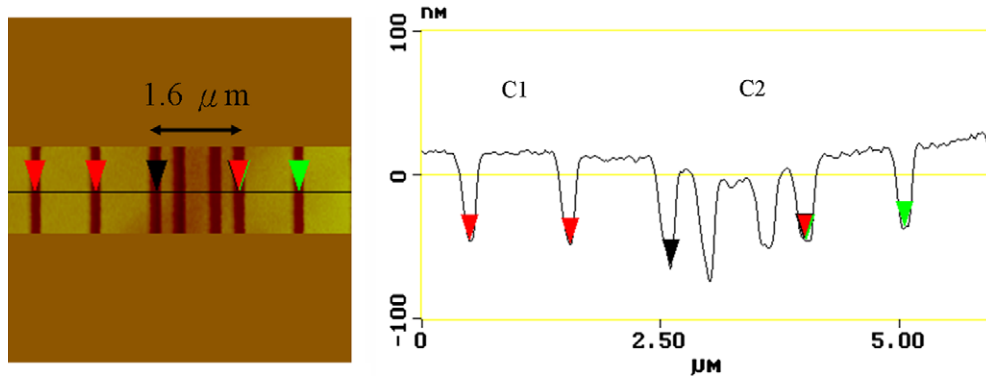


Fig. 3. AFM micrograph of the smallest stitching error, which is 1.6 μm by line to line. C1 is the spacing of grating (1 μm), C2 is stitching errors (1.6 μm) between two different grating period.

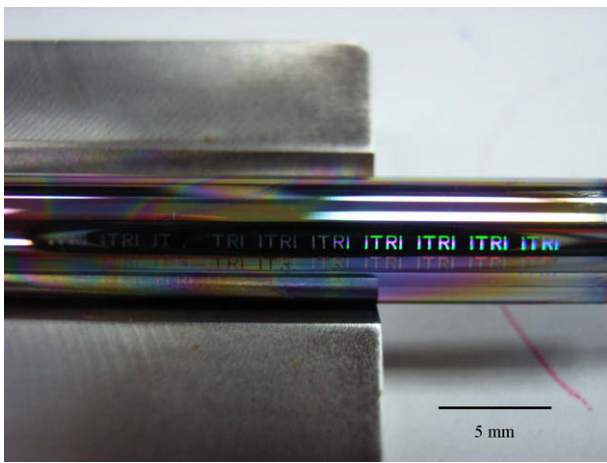


Fig. 4. Couples of ITRI patterns on the cylindrical roller, of which diameter is 5 mm.

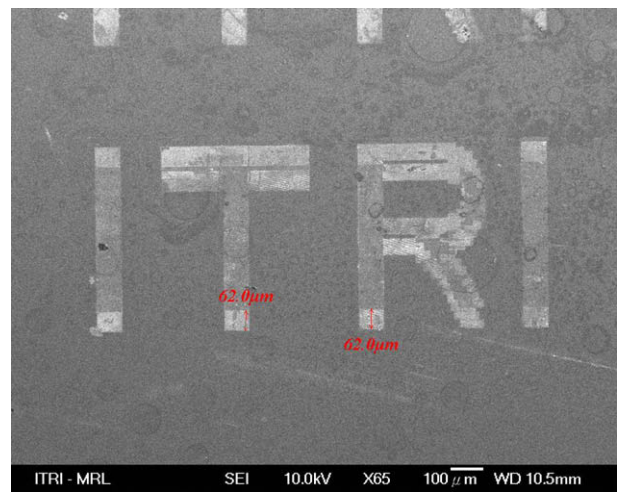


Fig. 5(a). SEM images of the ITRI pattern on the cylindrical roller Ni template.

distance of EBL could be affected by different heights. At the meantime, as the axle rotating at higher rotating speed, it caused larger z-axis vibration. In other words, displacement phenomenon of the roller occurred that added up to the stitching errors. Although the pattern size and stitching error for these demonstrations were about 200 nm and 1.6 μm, respectively, they could be reduced through a couple of optimization factors, such as dosage of EBL, the height relative to surface of R-axis stage, and R-axis rotation speed. Fig. 4 shows the couples of “ITRI” character patterns on the cylindrical roller with a diameter of 5 mm. The surface

flatness was great that meant the slurry had high energy during the polishing process. Besides, it showed the high speed axial system has better stability at 25,000 r.p.m. coating speed. It means the uniformity of photo-resist thickness on the roller is well achieved. The “ITRI” character pattern over the cylindrical roller had been electroforming after EBL exposure in order to shape the Ni template as shown in Figs. 5(a) and (c). Table 1 shows the composition of the solution and operating parameters. Electroforming process is carried out in the PTFE tank with a chemical solution at elevated

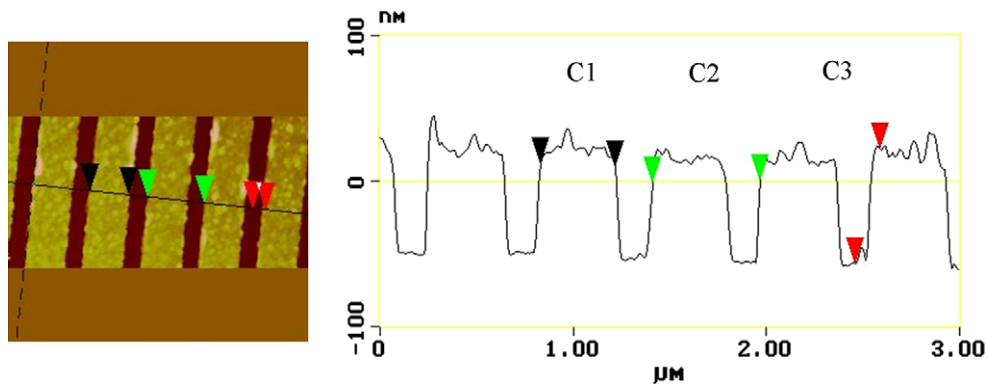


Fig. 5(b). AFM images of the structure on the Ni template: C1 is the distance of Ni template (386 nm), C2 is the pitch of Ni template (562 nm), C3 is depth of Ni (80 nm).

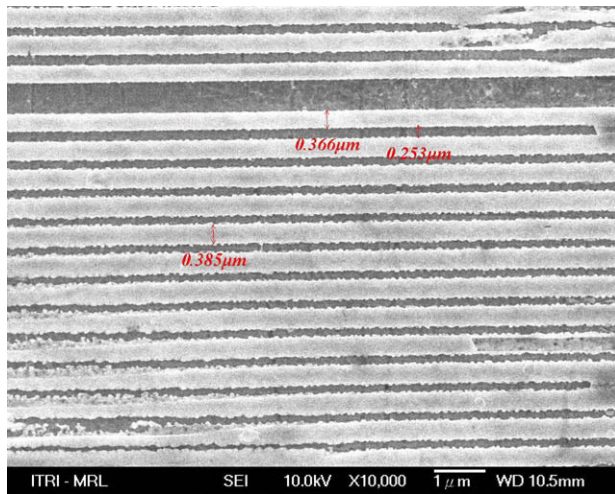


Fig. 5(c). SEM photograph of the Ni template.

Table 1

Composition of the chemical solution and operating parameters used in an electroforming process.

Electroforming solution	
Composition	Unit (gL ⁻¹)
DMBA	1
NiCl ₂	7
CoSO ₄	1
NaOAc	1.5
PH	4.8
Solution temperature	60 °C

temperature. The final thickness of the nano-structure Ni mold is according to the deposition time, and the normal thickness in this study is 80 nm or so. It was proven by AFM, as shown in Fig. 5(b). The mold has been further tempered to release the residual stress in the nitrogen ambience, which avoided the warp and brittleness

of the template. The system in this study may support 3D nano-field research and also has significant impact in other fields.

4. Conclusions

This work presents a novel approach for fabricating arrays nano-grating structure and “ITRI” character patterns using the electron beam lithography (EBL) and electroforming process. Our in-house made polisher, photo-resist coating, and R-axis facility enable the nano-patterns on the mini roller by EBL. The smallest width of arrays circle grating is about 200 nm and a pitch of about 400 nm. The width depends on the dosage of EBL and curvature of roller. Additionally, the stitching error of in-house made R-axis drive apparatus was investigated. The stitching errors decreased from 30 μm to 1.6 μm as the height decreased from 4.5 mm to 0.5 mm. Last but not least, the Ni template had been completed and the normal thickness is 80 nm or so. A study of nano-imprinting is currently continued in order to transfer the “ITRI” character pattern after the electroforming process.

References

- [1] A.G. Lopez, H.G. Craighead, *Opt. Lett.* 15 (1998) 1627.
- [2] W. Yu, K. Satoh, H. Kikuta, T. Konishi, T. Yotsuya, *Jpn. J. Appl. Phys.* 43 (2004) L439.
- [3] Y. Kanamori, K. Kobayashi, H. Yugami, K. Hane, *Jpn. J. Appl. Phys.* 42 (2003) 4020.
- [4] C. Heine, R.H. Morf, *Appl. Opt.* 34 (1995) 2476.
- [5] A. Gombert et al., *Opt. Eng.* 43 (2004) 2525.
- [6] V. Boerner, S. Abbott, B. Blasi, A. Gombert, W. Hobfeld, *SID 03 Dig.*, 68 (2003).
- [7] M. Ishimori, Y. Kanamori, M. Sasaki, K.J. Hane, *J. Appl. Phys.* 41 (2003) 4346.
- [8] T. Tsuchiya, O. Tabata, J. Sakata, Y. Taga, *J. Microelectromech. Syst.* 7 (1998) 106.
- [9] H. Sato, T. Kakimra, J.S. Go, S. Shoji, *Proc. IEEE MEMS* (2003) 223.
- [10] V. Kudryashov, X.-C. Yuan, W.-C. Cheong, K. Radharkrishnan, *Microelectron. Eng.* 67–68 (2003) 306.
- [11] B. Bilenberg, S. Jacobsen, M.S. Schmidt, L.H.D. Skjolding, P. Shi, P. Boggild, J.O. Tegenfeldt, A. Kristensen, *Microelectron. Eng.* 83 (2006) 1609.
- [12] M. Hecke, W.K. Schomburg, *J. Micromech. Microeng.* 14 (2004) R1–14.
- [13] M.T. Gale et al., *Opt. Laser Eng.* 43 (2005) 373.
- [14] K. Yamazaki, H. Namatsu, *Microelectron. Eng.* 73–74 (2004) 85.
- [15] S.L. Lv, Z.T. Song, S.L. Feng, *Microelectron. J.* 39 (2008) 1126.
- [16] S.Y. Chou, P.R. Krauss, P.J. Renstrom, *Appl. Phys. Lett.* 67 (1995) 3114.
- [17] S.Y. Chou, P.R. Krauss, P.J. Renstrom, *J. Vac. Sci. Technol. B* 14 (1996) 4129.